JOURNAL OF VIROLOGY, Oct. 2009, p. 9957–9969 Vol. 83, No. 19
0022-538X/09/$08.00+0 doi:10.1128/JVI.00508-09

Genetic Inactivation of Poliovirus Infectivity by Increasing the Frequencies of CpG and UpA Dinucleotides within and across Synonymous Capsid Region Codons▽†

Cara C. Burns,* Ray Campagnoli, Jing Shaw, Annelet Vincent, Jaume Jorba, and Olen Kew

Division of Viral Diseases, National Center for Immunization and Respiratory Diseases, Centers for Disease Control and Prevention, Atlanta, Georgia 30333

Received 11 March 2009/Accepted 9 July 2009

Replicative fitness of poliovirus can be modulated systematically by replacement of preferred capsid region codons with synonymous unpreferred codons. To determine the key genetic contributors to fitness reduction, we introduced different sets of synonymous codons into the capsid coding region of an infectious clone derived from the type 2 prototype strain MEF-1. Replicative fitness in HeLa cells, measured by plaque areas and virus yields in single-step growth experiments, decreased sharply with increased frequencies of the dinucleotides CpG (suppressed in higher eukaryotes and most RNA viruses) and UpA (suppressed nearly universally). Replacement of MEF-1 capsid codons with the corresponding codons from another type 2 prototype strain (Lansing), a randomization of MEF-1 synonymous codons, increased the %G+C without increasing CpG, and reductions in the effective number of codons used had much smaller individual effects on fitness. Poliovirus fitness was reduced to the threshold of viability when CpG and UpA dinucleotides were saturated within and across synonymous codons of a capsid region interval representing only ~9% of the total genome. Codon replacements were associated with moderate decreases in total virion production but large decreases in the specific infectivities of intact poliovirions and viral RNAs. Replication of codon replacement viruses, but not MEF-1, was temperature sensitive at 39.5°C. Synthesis and processing of viral intracellular proteins were largely unaltered in most codon replacement constructs. Replacement of natural codons with synonymous codons with increased frequencies of CpG and UpA dinucleotides may offer a general approach to the development of attenuated vaccines with well-defined antigenicities and very high genetic stabilities.

Diversification of genomic sequences is constrained in all biological systems. At the level of primary sequences, the range of variability in coding regions is restricted by the codon usage bias (CUB), whereby a subset of synonymous codons are preferentially used in translation (24, 53, 69). The intensity of the CUB and the specific set of preferred codons vary widely across biological systems (39). Intertwined with the CUB is the suppression of the dinucleotides CpG and TpA (or UpA in RNA viruses) in the genomes of higher eukaryotes (4, 7, 26, 61) and many of their RNA viruses and small DNA viruses (28, 49). Variation in the primary sequences of RNA virus genomes is further constrained by requirements to maintain essential secondary and higher-order structures (42, 54, 68).

We previously described the modulation of the replicative fitness of the Sabin type 2 oral poliovirus vaccine (OPV) strain (Sabin 2) by systematically changing the CUB in the capsid region, replacing the naturally occurring preferred codons with an unpreferred synonymous codon (isocodon) for each of nine amino acids (8). We called our approach "codon deoptimization" to contrast with the process of codon optimization, which is frequently used to maximize expression of foreign proteins in heterologous host systems (1, 27, 70). Apart from its potential application to development of improved poliovirus vaccines (8, 13, 38), experimental investigations of codon deoptimization directly test the relationships between replicative fitness, the extent of CUB, and the intensity of CpG and UpA suppression. As a model system for such studies, polioviruses offer several favorable properties, including (i) intrinsically high error rates for the poliovirus RNA-dependent RNA polymerase (2, 14, 16, 65), (ii) very high evolution rates (25), (iii) short generation times (8 to 10 h) and large progeny yields of prototype polioviruses, and (iv) well-developed reverse genetics (9).

In this report, we extend our codon deoptimization strategy to the type 2 wild poliovirus prototype strain MEF-1. As before, we restricted our replacement of synonymous codons to the capsid coding region, which encodes two of the defining properties of polioviruses, namely, (i) the capacity to bind the CD155 poliovirus receptor (PVR) (23) and (ii) the poliovirus type-specific neutralizing antigenic sites (35). No changes were made to the flanking 5′-untranslated region and noncapsid region sequences, as they contain essential secondary structural elements (42, 54, 68) and are frequently exchanged out by recombination during circulation of poliovirus in human populations (20, 30, 32). MEF-1 was selected because of its high fitness level (hence, its use as the type 2 component of the inactivated poliovirus vaccine [IPV]) and because of its neurovirulence for humans (15), for nontransgenic mice (52), and for transgenic mice expressing the PVR (71). Type 2 polioviruses were selected first for study because the Sabin 2 OPV

* Corresponding author. Mailing address: Polio and Picornavirus Branch, G-10, Division of Viral Diseases, National Center for Immunization and Respiratory Diseases, Centers for Disease Control and Prevention, 1600 Clifton Rd., N.E., Atlanta, GA 30333. Phone: (404) 639-5499. Fax: (404) 639-4011. E-mail: CBurns@cdc.gov.

† Supplemental material for this article may be found at http://jvi.asm.org/.

▽ Published ahead of print on 15 July 2009.

strain is most frequently associated with vaccine-associated paralytic poliomyelitis in contacts of OPV recipients (57, 59), with prolonged excretion of immunodeficiency-associated vaccine-derived polioviruses (VDPVs) (10, 31, 60), and with the emergence of circulating VDPVs in areas of low OPV coverage (10, 31).

Consistent with our previous findings, the fitness of MEF-1 decreased in proportion to the total number of synonymous replacement codons. Fitness was reduced most efficiently by increasing the frequencies of CpG and UpA dinucleotides within and across synonymous codons. Saturation of CpG and UpA in a small capsid interval (representing only ~9% of the genome) reduced fitness to the threshold of viability, even though the MEF-1 amino acid sequence was unaltered. The most prominent biological effect of deoptimization of codon usage and the large-scale incorporation of CpG and UpA was a sharp reduction in virus specific infectivities. In contrast, translation and processing of viral proteins and yields of intact virus particles with native antigenicities were reduced only moderately by increased CpG and UpA frequencies. Codon deoptimization with concurrent increases in the frequencies of CpG and/or UpA dinucleotides in RNA virus genomes may provide a novel general approach to the rational design of improved attenuated vaccines with predictable and stable genetic properties.

MATERIALS AND METHODS

Virus, cells, and plaque assay. The type 2 IPV seed strain MEF-1, a gift of Connaught Laboratories (Toronto, Ontario, Canada), was received in 1960 as their lot 55. Virus was subsequently passaged twice in primary rhesus monkey kidney cells and once in FL cells (ATCC CCL-62), with a final passage in L20B cells (mouse L cells expressing the PVR [44]), before extraction of RNA to produce the infectious MEF-1 cDNA clone. Subsequent virus growth experiments were done with suspension cultures of HeLa S3 cells (ATCC CCL-2.2), monolayer cultures of HeLa cells (ATCC CCL-2), or RD cell (ATCC CCL-136) monolayers as described below. Suspension cultures of HeLa S3 cells were used for single-step growth experiments; monolayer cultures of HeLa cells were used in the plaque assays and competition experiments and for production of radiolabeled virus-specific proteins in infected cells; and RD cells, which had the highest sensitivity to poliovirus and supported the highest infectivity yields, were used in the transfection experiments and in measurements of specific infectivities. Incubations were done at 37°C unless otherwise indicated. Plaque assays were performed on HeLa cell monolayers as previously described (8).

Preparation of infectious MEF-1 clones. Infectious MEF-1 clones were prepared by minor modification of our previously described methods (8). The primer for reverse transcription was S2-7439A-C [TCCTAAGC$(T)_{30}$CTCCGA ATTAAAGAAAAATTTACCCCTAC], which was also used in the subsequent PCR amplification in combination with primer S2-1S-Pst (AATCTGCAGTAA TACGACTCACTATAGGTTAAAACAGCTCTGGGGTTG). Purified PCR products were digested with the restriction enzymes HindIII and PstI (Roche Applied Science, Indianapolis, IN), ligated into pUC19 plasmids, and transformed into SoloPack Gold supercompetent *Escherichia coli* cells (Stratagene, La Jolla, CA). Sequences of the inserts were determined by cycle sequencing using an automated DNA sequencer (Applied Biosystems, Foster City, CA). Appropriate restriction fragments of different clones were subcloned to generate a full-length cDNA clone with the fewest mutations. Base substitutions were corrected by using a QuikChange multisite-directed mutagenesis kit (Stratagene) as described previously (8). An AgeI site was introduced by QuikChange mutagenesis into the infectious MEF-1 clone by replacement of the codon pair TTG-CCA with TTA-CCG just downstream of the VP2-VP3 junction.

Virus preparation. In vitro transcripts of viral RNA were transfected into semiconfluent RD cell monolayers by using Tfx-20 reagent (Promega, Madison, WI) essentially as described previously (8). A complete cytopathic effect was observed for most viruses after incubation at 37°C for 22 h, at which time 400 μl from each transfected well was transferred to a confluent RD cell monolayer in a 75-cm^2 flask containing complete minimal essential medium. In this second passage, complete cytopathic effect was observed after 24 h at 37°C for all but the most highly modified viruses (abc_0, ABc_{10}, ABc_{11}, and ABc_{12}), which were incubated for an additional 24 to 48 h. The sequences of all virus stocks were verified by in vitro amplification of large overlapping fragments and sequence analysis of the PCR products (8).

Construction of recombinant cDNA plasmids by assembly PCR and exchange of mutagenesis cassettes. Multiple base substitutions were introduced by assembly PCR (55) essentially as previously described (8). Clones were screened by sequencing; clones with no (or minimal) errors were spliced together at restriction endonuclease sites, and any remaining errors were repaired with Multi-QuikChange.

Design of constructs. Clones were designed using logical functions within Microsoft Excel. Nucleic acid and amino acid sequences were placed vertically in an Excel worksheet, and different sets of logical functions were developed for codon and dinucleotide usage for each clone design. Unwanted restriction sites were removed, and needed restriction sites were added manually.

Single-step growth experiments. Single-step growth experiments were performed by infection of HeLa S3 suspension cells at a multiplicity of infection (MOI) of 10 PFU/cell as described previously (8).

Preparation of purified virions. Viruses were propagated in RD cells, liberated by freeze-thawing, and concentrated by precipitation with polyethylene glycol 6000. Virions were purified by pelleting, isopycnic banding in CsCl, and repelleting (8, 40). The number of virus particles in each preparation recovered from the CsCl band with a buoyant density of 1.34 g/ml was calculated from the absorbance at 260 nm, using the relationship 9.4×10^{12} virions per optical density unit at 260 nm (51).

Preparation of radiolabeled viral proteins. Virus-specific proteins were radiolabeled with [^{35}S]methionine during infection of HeLa cell monolayers (labeling times were at 4 to 7 h or 7 to 10 h postinfection) at 37°C (8). We used concentrated purified virus for all infections to obtain a uniform MOI of 25. Labeled viral proteins were separated by sodium dodecyl sulfate-10% polyacrylamide gel electrophoresis (SDS-PAGE) and visualized by autoradiography as described previously (8).

Infectivities of RNA transcripts. Transcripts were transfected onto HeLa cell monolayers as described previously (8). RNA concentrations were determined from the absorbance at 260 nm.

Calculation of N_C, CAI, and CPB. The effective number of codons used (N_C; values range from 20 [extreme CUB; only one codon used for each amino acid] to 61 [no CUB]) and the codon adaptation index (CAI; the fraction of codons matching those of one or more reference sequences [usually highly expressed genes]) were calculated by using the program CodonW (http://codonw.sourceforge.net/). The MEF-1 capsid region codon usage was used as a reference for calculating the CAI. The Anaconda program (43) was used to determine the codon pair usage, and these values were used to calculate the codon pair bias score (CPB score; negative values indicate a predominance of unpreferred codon pairs, and positive values identify a predominance of preferred codon pairs), using the formula and tables for codon pair scores for the full complement of human open reading frames described by Coleman et al. (13).

Antigenic characterization. The type- and intratype-specific properties of virus constructs were determined in enzyme-linked immunosorbent assays, using highly specific cross-absorbed antisera as previously described (64, 71).

Kinetics of thermal inactivation of purified virions. Undiluted clarified infected cell culture lysates (50 μl) were dispensed into thin-walled tubes and transferred to a thermocycler preset to 46°C. At 5, 10, 20, and 30 min of incubation at 46°C, duplicate tubes for each virus were transferred to ice. Residual infectivity was determined by plaque assay, with samples incubated only on ice for 30 min (zero time) used as a reference.

Nucleotide sequence accession numbers. Complete genomic sequences of the MEF-1 seed strain and recombinant virus constructs *ABC* and abc_0, in addition to cassette *C* inserts c_1 to c_{12}, were submitted to the GenBank library under accession numbers CS406482 to CS406488 and FJ816703 to FJ816714.

RESULTS

Initial strategy for codon deoptimization in MEF-1. Our initial experiments for deoptimization of codons in the P1/capsid region of MEF-1 followed the approach we used previously with the Sabin 2 strain (8). The original capsid region codons of MEF-1 were replaced with the following unpreferred codons: CUU for Leu, AGC for Ser, CGG for Arg, CCG for Pro, GUC for Val, ACG for Thr, GCG for Ala, GGU

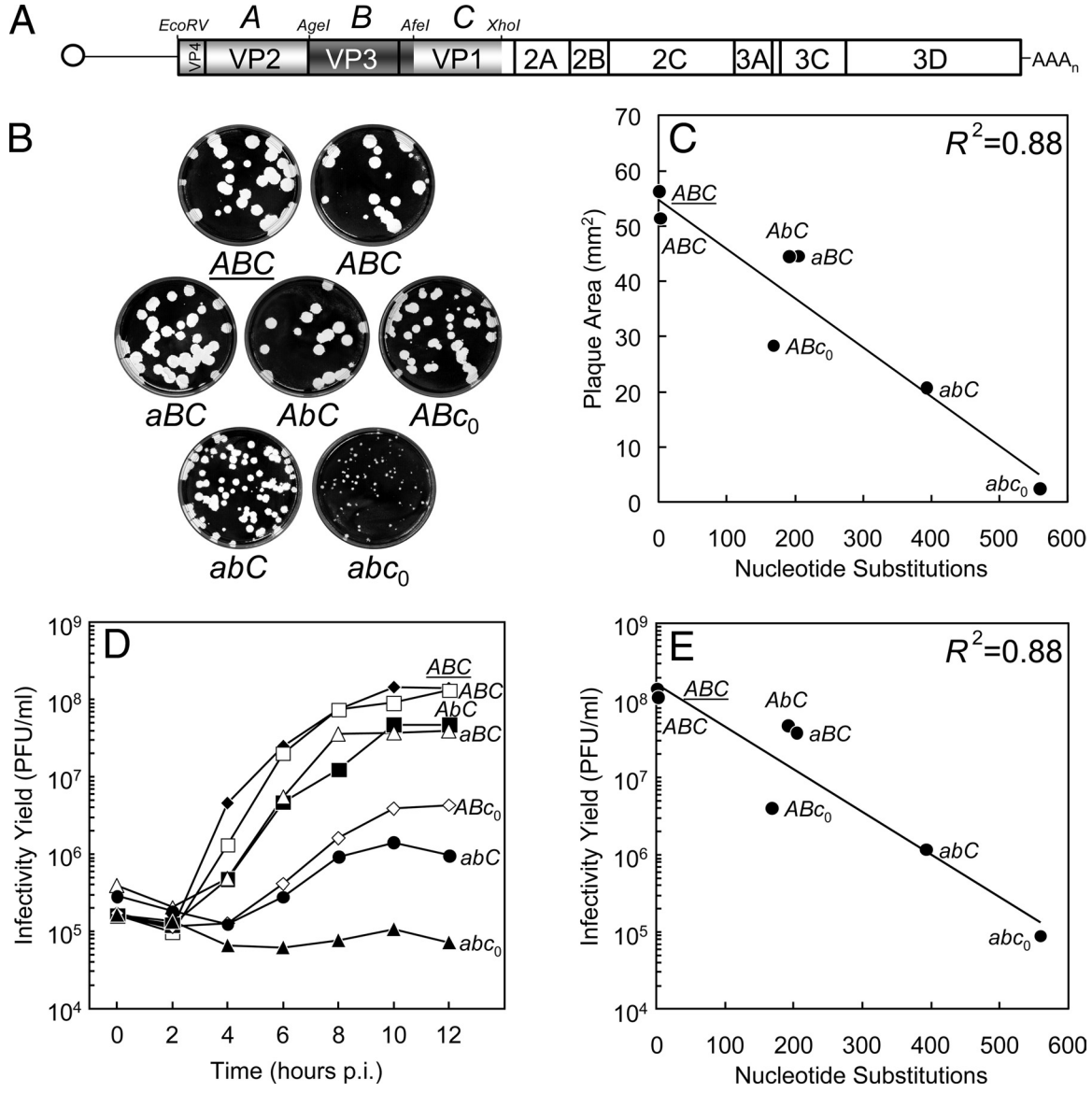

FIG. 1. (A) MEF-1 codon replacement constructs aligned with a schematic of the poliovirus genome, with the single open reading frame represented by an open rectangle, flanked by the 5′- and 3′-untranslated regions, represented as lines. Bounding restriction endonuclease sites and locations of codon replacement cassettes (*A*, EcoRV-AgeI fragment [nt 748 to 1773; 1,026 nt]; *B*, AgeI-AfeI fragment [nt 1774 to 2610; 837 nt]; and *C*, AfeI-XhoI fragment [nt 2611 to 3300; 690 nt]) are indicated above the capsid region. Unmodified cassettes are indicated by italicized capital letters. *ABC* nucleotide sequences completely matched the MEF-1 sequence; *ABC* had two synonymous substitutions introduced to generate an AgeI site. (B) Plaque morphologies on HeLa cell monolayers (37°C, 60 h, 10-cm plates). Relative amounts of infected cell culture lysates yielding the plaques shown in each dish were as follows: *ABC*, 1; *ABC*, 0.1; *aBC*, 1; *AbC*, 1; ABc_0, 1; *abC*, 10; and abc_0, 4,000. (C) Mean plaque areas as a function of the number of nucleotide substitutions in the capsid region. (D) Growth properties of different virus constructs in single-step growth experiments in HeLa S3 cells (37°C). Single-step growth experiments were performed as described in Materials and Methods, and virus yields were determined by plaque assay. One milliliter of culture contained 2×10^6 HeLa S3 cells. (E) Virus yields (averages for 10-h and 12-h time points) of the single-step growth experiments as a function of the total number of nucleotide substitutions in the capsid region.

for Gly, and AUC for Ile. Replacement codons were introduced into a full-length infectious MEF-1 cDNA clone within an interval (nucleotide [nt] positions 748 to 3300) spanning all but the last 28 codons of the capsid region (Fig. 1A). The capsid interval was divided into three mutagenesis cassettes, namely, *A*, *B*, and *C* (Fig. 1A). Within each cassette, synonymous codons for the nine amino acids were replaced at all but seven positions. Unmodified cassettes are identified by italicized capital letters, and codon replacement cassettes are identified by italicized lowercase letters. Different cassette *C* constructs (see the following sections) are identified by subscripts. The following two reference wild-type MEF-1 capsid constructs were prepared: *ABC*, whose nucleotide sequence completely matched the consensus sequence of the MEF-1 seed strain, and *ABC*, into which two synonymous nucleotide changes were introduced to generate an AgeI restriction site between the *A* and *B* cassettes.

The predicted amino acid sequences were unaltered in all

codon replacement constructs, but mono-, di-, and trinucleotide (codon) frequencies were dramatically altered. Compared with the *ABC* reference sequence, virus construct abc_0 had 557 nucleotide substitutions that replaced nearly half (439/879 codons; 49.9%) of the capsid region codons. The N_C (69) in the capsid region fell from 55.2 (*ABC*) to 29.0 (abc_0), the CAI (a measure of the frequency of preferred codon usage in a gene) (53) fell from 0.78 to 0.52, the number of CpG dinucleotides rose from 94 to 303, and the %G+C increased from 48.6% to 56.6%.

Replicative fitness decreases with increasing numbers of synonymous unpreferred codons. We assessed the replicative fitness of the virus constructs by measuring plaque areas and by determining virus growth kinetics and yields in single-step growth experiments. Mean plaque areas decreased 20-fold (from ~51 mm^2 [*ABC*] to ~2.5 mm^2 [abc_0]), in approximate proportion to the number of nucleotide substitutions (and unpreferred codons) in the capsid region (Fig. 1B and C). Enumeration of plaques and measurement of mean plaque areas were especially difficult with virus construct abc_0 because the plaques were minute and heterogeneous in diameter (Fig. 1B), likely resulting in an undercount of plaque numbers and an overestimate of mean plaque areas. We cannot exclude the possibility that the larger plaques were from higher-fitness variants, but heterogeneity of plaque areas was also observed with unmodified constructs (Fig. 1B).

Plaque yields from single-step growth experiments varied over an ~1,500-fold range, from ~73 PFU/cell (*ABC*) to ~0.05 PFU/cell (abc_0) (Fig. 1D and E). Time courses for virus production slowed with increased numbers of replacement codons. Single-step growth yields of *abC* virus were only ~4-fold higher than input, and the yields of abc_0 virus were ~50% of input. As observed with Sabin 2 (8), codon replacements in the VP1 region (cassette *C*) appeared to have proportionately greater effects than replacements elsewhere in the capsid region.

The fitness of the MEF-1 abc_0 virus was very low, even lower than the fitness of the homologous Sabin 2 *abcd* virus (8). When MEF-1 abc_0 virus and Sabin 2 *abcd* virus were cultured together in HeLa cells (35°C) at an initial infectivity ratio of 10:1, Sabin 2 *abcd* overgrew MEF-1 abc_0 within five passages, as the only virus genome detectable by bulk sequencing was that of Sabin 2 *abcd* (data not shown). Under similar culture conditions with an initial infectivity ratio of 1:1, MEF-1 *ABC* virus readily overgrew Sabin 2 *ABCD* virus, as expected from the relative growth properties of their original parental strains. Nonetheless, with separate cultures, MEF-1 abc_0 infectivity was retained through five serial passages in HeLa cells.

Genetic contributors to reduced fitness. Our initial codon deoptimization strategy simultaneously introduced multiple changes into the natural MEF-1 sequence. Because many of these changes are interrelated, it is not possible to completely separate and individually test the contributions of each change to the overall phenotype. To approach this problem, we measured the fitness of the following 14 different virus constructs with synonymous codon replacements that applied different genetic parameters for substitution into VP1 cassette *C*: *ABC* (MEF-1 reference), ABc_0 (original nine codon choices described above), ABc_1 (MEF-1 sequences replaced by corresponding sequences of the unrelated wild-type 2 strain Lansing), ABc_2 (randomized synonymous MEF-1 cassette *C* codons), ABc_3 (original nine codon choices, but incorporating only changes that increased CpG), ABc_4 (original nine codon choices, excluding changes that increased CpG), ABc_5 (alternative rare codons with low or equivalent %G+C), ABc_6 (increased %G+C, with CpG frequency unchanged and UpA frequency minimized), ABc_7 (maximum CpG frequency across codon junctions [codon positions 3 and 1; $CpG_{3\text{-}1}$]), ABc_8 (maximum CpG frequency; priority to $CpG_{1\text{-}2}$, then $CpG_{3\text{-}1}$, then $CpG_{2\text{-}3}$), ABc_9 (maximum UpA frequency; priority to $UpA_{3\text{-}1}$ and then $UpA_{2\text{-}3}$), ABc_{10} (maximum CpG frequency and then maximum UpA frequency; priority to $CpG_{1\text{-}2}$, then $CpG_{3\text{-}1}$, then $CpG_{2\text{-}3}$ and to $UpA_{3\text{-}1}$ and then $UpA_{2\text{-}3}$), ABc_{11} (maximum UpA frequency and then maximum CpG frequency; priority to $UpA_{3\text{-}1}$ and then $UpA_{2\text{-}3}$ and to $CpG_{1\text{-}2}$, then $CpG_{3\text{-}1}$, then $CpG_{2\text{-}3}$), ABc_{12} (codon choices selected by Mueller et al. [38]; degenerate codons for 18 amino acids were recoded to a single corresponding unpreferred isocodon, with maximum CpG and UpA frequencies within codons, with priority to $CpG_{1\text{-}2}$ and then $CpG_{2\text{-}3}$ and to $UpA_{2\text{-}3}$ and then $UpA_{3\text{-}1}$) (Table 1; Fig. 2; see Table S1 in the supplemental material). In several constructs with increased CpG or UpA (ABc_7 to ABc_{11}), CpG and UpA dinucleotides already present in MEF-1 were left unchanged. Virus constructs with modifications in cassette *C* (in an unmodified MEF-1 genetic background) were selected for comparison because of the proportionately greater effects of synonymous codon replacements in VP1 (Fig. 1C and E) (8). Among the 14 different cassettes, the number of nucleotide substitutions ranged from 0 to 171, the number of altered codons ranged from 0 to 160, the number of CpG dinucleotides ranged from 22 to 133, the number of UpA dinucleotides ranged from 13 to 112, %G+C ranged from 40.1% to 61.6%, N_C ranged from 20.2 to 53.3, the CAI ranged from 0.45 to 0.78, and the CPB score ranged from −0.37 to +0.17 (Table 1; Fig. 2; see Table S1 in the supplemental material). The relationships between fitness, measured by plaque areas (all 14 constructs) (Fig. 3A), and infectivity yields in single-step growth experiments (12 constructs) (Fig. 3B) were plotted as functions of the various genetic parameters (Fig. 4 and 5; Table 2).

(i) Total nucleotide substitutions, total altered codons, and %G+C. Fitness was only weakly correlated with total nucleotide substitutions (Fig. 4A and 5A) and total altered codons (Fig. 2, 4B, and 5B; see Table S1 in the supplemental material). For example, construct ABc_2 (randomized synonymous cassette *C* codons) had 153 substitutions and 138 altered codons (other parameters were similar to those of *ABC*) but only a small reduction in fitness. Elevated %G+C in cassette *C* alone (i.e., without increased CpG) had no effect on fitness, as the points in the regression plots were widely scattered, with no discernible trend (Fig. 4C and 5C). For example, the fitness of virus construct ABc_6 (%G+C in cassette *C* = 61.6%) was similar to that of unmodified MEF-1 (%G+C = 47.1%).

(ii) N_C, CAI, and CPB. Fitness was only weakly correlated with N_C (Fig. 4D and 5D). A stronger positive correlation was observed between fitness and the CAI, although there was substantial point scatter (Fig. 4E and 5E). Fitness was positively correlated with the CPB, but again with point scatter (Fig. 4F and 5F). For example, construct ABc_{12} (CPB score = −0.08) had minute plaques, whereas constructs ABc_2 and

TABLE 1. Genetic properties of cassette *C* codon replacement virus constructs

Virus construct[a]	Cassette *C* properties	No. of nt substitutions	No. of altered codons	%G+C	N_C[b]	CAI[c]	CPB[d]	No. of dinucleotides at indicated codon positions							
								CpG				UpA			
								All	1-2	2-3	3-1	All	1-2	2-3	3-1
ABC	MEF-1 reference sequence	0	0	47.1	53.3	0.78	0.00	28	7	10	11	36	13	12	11
ABc_0	Original nine replacement codons	166	124	57.7	26.7	0.52	−0.07	90	13	55	22	26	13	0	13
ABc_1	MEF-1 codons replaced by Lansing codons	100	98	49.3	51.3	0.75	−0.03	31	7	12	12	31	13	10	8
ABc_2	Randomized synonymous codons	153	138	47.1	53.3	0.78	−0.08	35	7	10	18	42	13	12	17
ABc_3	ABc_0 subset with added CpG	76	63	54.9	40.4	0.61	−0.13	91	13	54	24	34	13	11	10
ABc_4	ABc_0 subset excluding added CpG	90	61	49.9	34.8	0.66	0.02	27	7	11	9	31	13	1	17
ABc_5	Codon replacements without increased %G+C[e]	160	121	47.2	26.6	0.54	−0.08	33	0	16	17	53	13	0	40
ABc_6	Increased %G+C; no CpG increase	100	98	61.6	30.9	0.72	0.17	28	7	10	11	13	13	0	0
ABc_7	CpG_{3-1}	53	49	53.3	52.0	0.73	−0.24	80	10	10	60	34	13	10	11
ABc_8	CpG_{1-2}, CpG_{3-1}, CpG_{2-3}[f]	110	103	59.3	37.6	0.57	−0.22	133	13	59	61	29	13	10	6
ABc_9	UpA_{3-1}, UpA_{2-3}	106	80	40.1	39.9	0.67	−0.12	22	4	4	14	112	13	36	63
ABc_{10}	CpG_{1-2}, CpG_{3-1}, CpG_{2-3}; UpA_{3-1}, UpA_{2-3}[g]	150	137	55.1	40.5	0.53	−0.37	133	13	58	62	64	13	24	27
ABc_{11}	UpA_{3-1}, UpA_{2-3}; CpG_{1-2}, CpG_{3-1}, CpG_{2-3}	158	131	46.7	44.6	0.62	−0.33	73	6	22	45	112	13	36	63
ABc_{12}	CpG_{1-2}, CpG_{2-3}; UpA_{2-3}, UpA_{3-1}	171	160	43.5	20.2	0.45	−0.08	87	13	74	0	75	13	43	19

[a] The cassette *C* sequences of the codon replacement constructs have been deposited in GenBank (accession numbers CS406482 to CS406488 and FJ816703 to FJ816714).
[b] Effective number of codons used (69).
[c] For cassette *C* nt 2611 to 3300 (53). The MEF-1 capsid region was used as a baseline reference.
[d] See reference 13. The CPB includes codons adjoining cassette *C*.
[e] A different set of unpreferred codons for the same nine amino acids targeted by ABc_0.
[f] Given in priority order of incorporation into cassette *C* (CpG_{1-2}, then CpG_{3-1}, then CpG_{2-3}).
[g] Given in priority order of incorporation into cassette *C* (CpG_{1-2}, then CpG_{3-1}, then CpG_{2-3} and UpA_{3-1} and then UpA_{2-3}).

ABc_5, with the equivalent CPB score of −0.08, had plaques that were only 20 to 30% smaller than those of the MEF-1 prototype (with comparably small reductions in infectivity yields) (Fig. 4F and 5F; Table 2).

(iii) CpG and UpA dinucleotides. Plaque areas and infectivity yields were negatively correlated with the number of CpG dinucleotides (Fig. 4G and 5G). The negative correlation with UpA was weaker (Fig. 4H and 5H), possibly because fewer constructs were specifically designed to test the effects of increased UpA. Part of the scatter in the regression plots could be attributed to different mechanisms contributing to fitness. For example, construct ABc_8 had a much higher fitness than ABc_{10}, despite having equivalent CpG frequencies (133) in cassette *C* (Tables 1 and 2), and construct ABc_9 had a much higher fitness than ABc_{11}, despite having equivalent UpA frequencies (112) in cassette *C* (Tables 1 and 2). An important difference within these pairs was that only one dinucleotide was maximized in the first virus construct, whereas both CpG and UpA were maximized in the second. Most notably, strong negative correlations ($R^2 = 0.87$ for plaque area and 0.65 for infectivity yields) were found between fitness and the combined number of CpG and UpA dinucleotides in cassette *C* (Fig. 4I and 5I). Nonetheless, the residual point scatter suggests that additional factors contribute to fitness. For example, construct ABc_8 gave much larger plaques than ABc_{12}, even though the total numbers of CpG and UpA dinucleotides were equivalent (162) for both viruses (Tables 1 and 2). Construct ABc_{12} differed from ABc_8 by having an additional 46 UpA dinucleotides (43 of which were UpA_{2-3}), reinforcing the views that the contributions of CpG and UpA are generally synergistic and that the positions of dinucleotide substitutions within (and across) codons may be important. Interestingly, construct ABc_{12} also had the most CpG_{2-3} substitutions, the most codon changes, and the lowest N_C and CAI values (Table 1).

Strong positive correlations were observed between fitness and the frequencies of CpA, UpG, and CpA-plus-UpG dinucleotides (Fig. 4J to L and 5J to L). Suppression of CpG and UpA in natural genomes is associated with an overrepresentation of CpA and UpG (7, 49), as the interconversions $CpG_{3-1} \leftrightarrow CpA_{3-1}$, $UpA_{3-1} \leftrightarrow CpA_{3-1}$, and $CpG_{2-3} \leftrightarrow CpA_{2-3}$ always generate synonymous codons, and $UpA_{2-3} \leftrightarrow UpG_{2-3}$ usually (with one exception) does. In our constructs, the natural CpA and UpG dinucleotides were replaced by CpG and UpA. Conversely, in higher-fitness revertants selected by serial passage of codon-deoptimized constructs, CpG and UpA dinucleotides were frequently replaced by CpA and UpG (8; our unpublished results).

Linear correlation coefficients (R^2) were generally lower for the plots of infectivity yields than for the plots of plaque areas, and the infectivity yield values for construct ABc_{10} were consistently below the trend lines (Fig. 5). Slopes of the trend lines were less steep for the infectivity yield plots than for the plaque area plots because constructs ABc_{11} and ABc_{12}, which had very low fitness, were not included in the infectivity yield analyses. Interestingly, constructs ABc_{10}, ABc_{11}, and ABc_{12}, in which the synonymous codon replacements were restricted to cassette *C*, had fitness levels that were similar to or lower than that of abc_0,

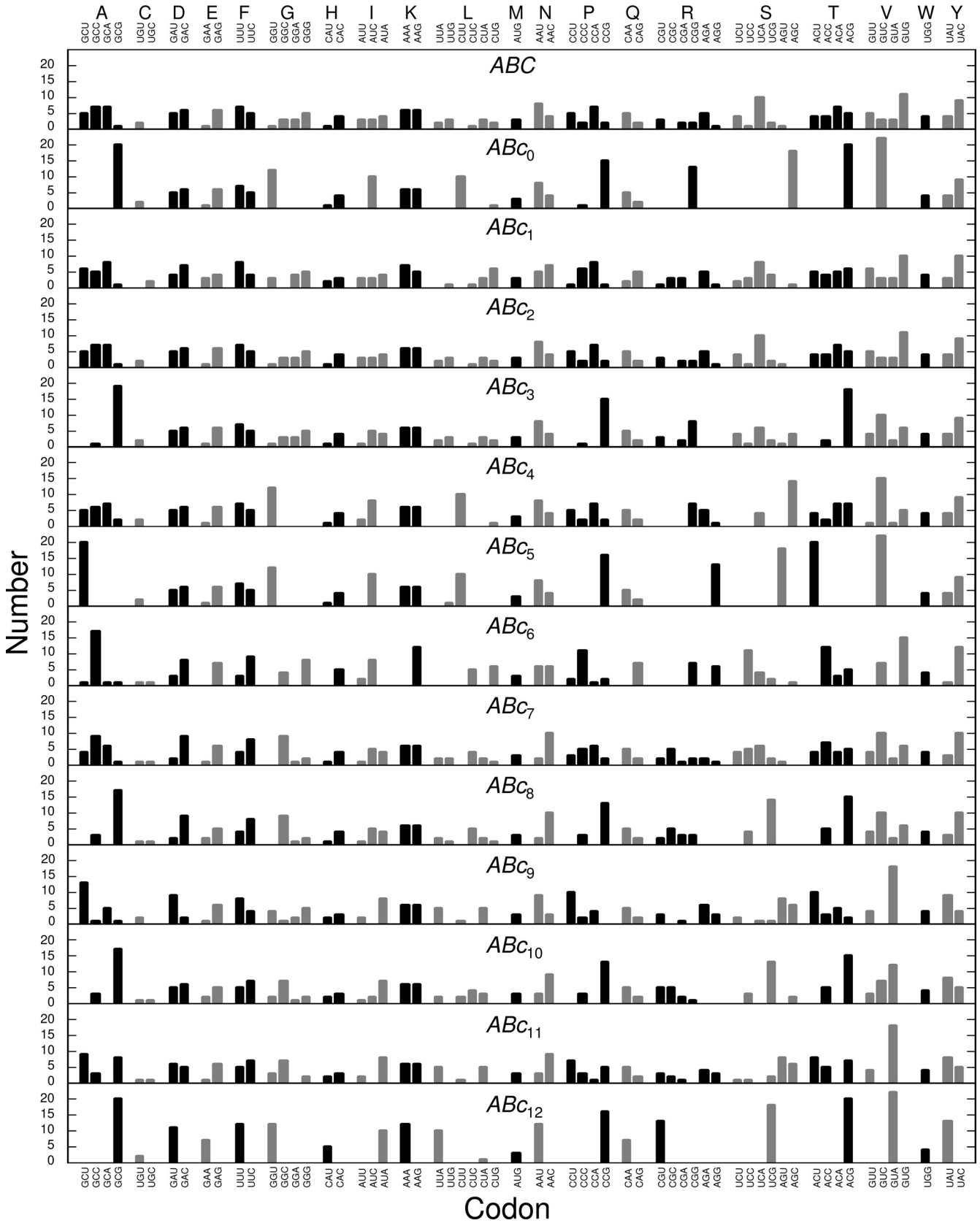

FIG. 2. Distribution of synonymous codon usage in cassette *C* of different virus constructs, described in Table 1 (also see Table S1 in the supplemental material). Encoded amino acids are identified by one-letter codes (top). Bars in graphs alternate between black and gray to facilitate visualization among amino acid codon sets.

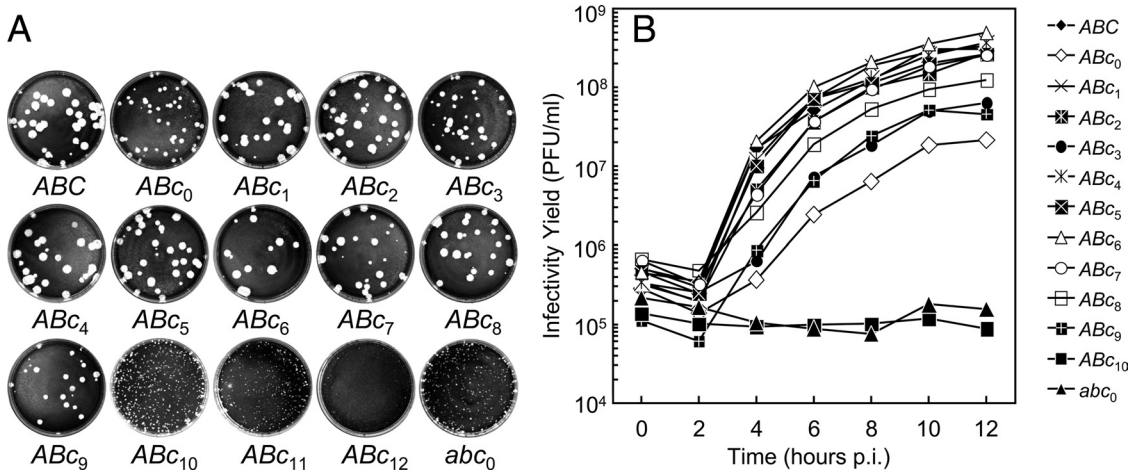

FIG. 3. (A) Plaque morphologies of constructs *ABC*, ABc_0 to ABc_{12}, and abc_0 on HeLa cell monolayers. Relative amounts of infected cell culture lysates yielding the plaques shown in each dish were as follows: *ABC*, 1; ABc_0, 4; ABc_1, 1; ABc_2, 1; ABc_3, 4; ABc_4, 1; ABc_5, 1; ABc_6, 1; ABc_7, 1; ABc_8, 1; ABc_9, 1; ABc_{10}, 1,600; ABc_{11}, 16,000; ABc_{12}, 160,000; and abc_0, 16,000. (B) Plaque yields of constructs *ABC*, ABc_0 to ABc_{10}, and abc_0 in single-step growth experiments in HeLa S3 cells.

in which codon replacements covered nearly the complete capsid region (Table 2).

Correlations between fitness and CAI improved ($R^2 = 0.71$ for plaque areas and 0.51 for infectivity yields) when the CAI of the human brain gene data set was used as a reference (38) but, nonetheless, remained lower than the corresponding correlations with CpG plus UpA.

Biological and physical properties of codon replacement virus constructs. Selected virus constructs from the preceding experiments were further characterized for their biological and physical properties.

(i) Virus particle yields and specific infectivities of purified virions. Virus constructs *ABC*, ABc_0, *abC*, and abc_0 were grown in RD cells, and virus particles were purified by pelleting through a sucrose cushion and isopycnic banding at 1.34 g/ml in CsCl gradients. Virus particle yields were determined from the absorbance at 260 nm, and virus infectivities were determined by plaque assay on HeLa monolayers. Purified infectious virions of all four virus constructs had SDS-PAGE profiles similar to those of MEF-1 (data not shown). Virus particle yields of the codon replacement constructs declined over a narrow (3- to 4-fold) range compared with that of *ABC*, whereas virus infectivities declined over a much wider (>100-fold) range (Fig. 6; Table 2). Virus infectivity yields were severalfold higher in RD cells than in HeLa S3 cells. The responses to increasing CpG-plus-UpA dinucleotides in the capsid region were nonlinear for both virus particle yields and virus infectivities, with infectivities falling off more rapidly than particle yields at high levels of substitution (Fig. 6).

(ii) Specific infectivities of viral RNAs. To determine if the decrease in specific infectivities of the virus constructs was an intrinsic property of the viral RNAs, we measured the specific infectivities of transcript RNAs from *ABC*, ABc_0, and abc_0 in a direct transfection/plaque assay. The specific infectivity of the *ABC* prototype RNA transcript was 344 PFU/ng RNA. The specific infectivity of the ABc_0 RNA (50 PFU/ng RNA) was 6.9-fold lower than that of *ABC* RNA (similar to the 2.8-fold lower specific infectivity of ABc_0 virions than that of *ABC* virions), and the specific infectivity of the abc_0 RNA (2.4 PFU/ng RNA) was 143-fold lower than that of *ABC* RNA (similar to the 93-fold lower specific infectivity of abc_0 virions than that of *ABC* virions). Plaque areas obtained under the equivalent incubation conditions of the direct transfection/plaque assays were similar to those initiated by the corresponding virus particles (data not shown).

(iii) Synthesis and processing of viral proteins in infected HeLa cells. We had previously shown that the efficiency of shutoff of host cell protein synthesis and the synthesis and processing of viral proteins were largely unaltered by restriction of codon usage in the Sabin 2 capsid region (8). We obtained similar results when we repeated these experiments with selected codon replacement MEF-1 constructs. The electrophoretic profiles of viral intracellular proteins labeled from 4 to 7 h postinfection in infected HeLa cells (MOI = 25) were similar for virus constructs *ABC*, ABc_0, abc_0, ABc_{10}, and ABc_{11} (Fig. 7). However, the profile for ABc_{11} showed somewhat weaker virus-specific protein bands and the profile for ABc_{12} showed both a higher background and weaker virus-specific bands. To test whether the high background in the ABc_{12} profile was attributable to a delayed time course of infection, the experiment was repeated with cells labeled from 7 to 10 h postinfection. The relative intensities of virus-specific protein bands were reduced for *ABC*, ABc_0, abc_0, ABc_{10}, and ABc_{11}, but the profiles were otherwise similar to those obtained with the 4- to 7-h labeling window (data not shown). The background remained high in the ABc_{12} profile, suggesting that shutoff of host protein synthesis by this virus construct was less rapid or incomplete, despite the large number ($\sim 10^6$) of input particles per cell. To obtain equivalent MOIs for all constructs, it was necessary to have high particle inputs for the low-fitness viruses. We do not believe that the similarities among the electrophoretic profiles are attributable to the higher particle inputs of the low-fitness viruses. In vitro translation experiments, programmed by equivalent quantities of unmodified and codon replacement RNAs encoding Sabin 2 (8) or MEF-1

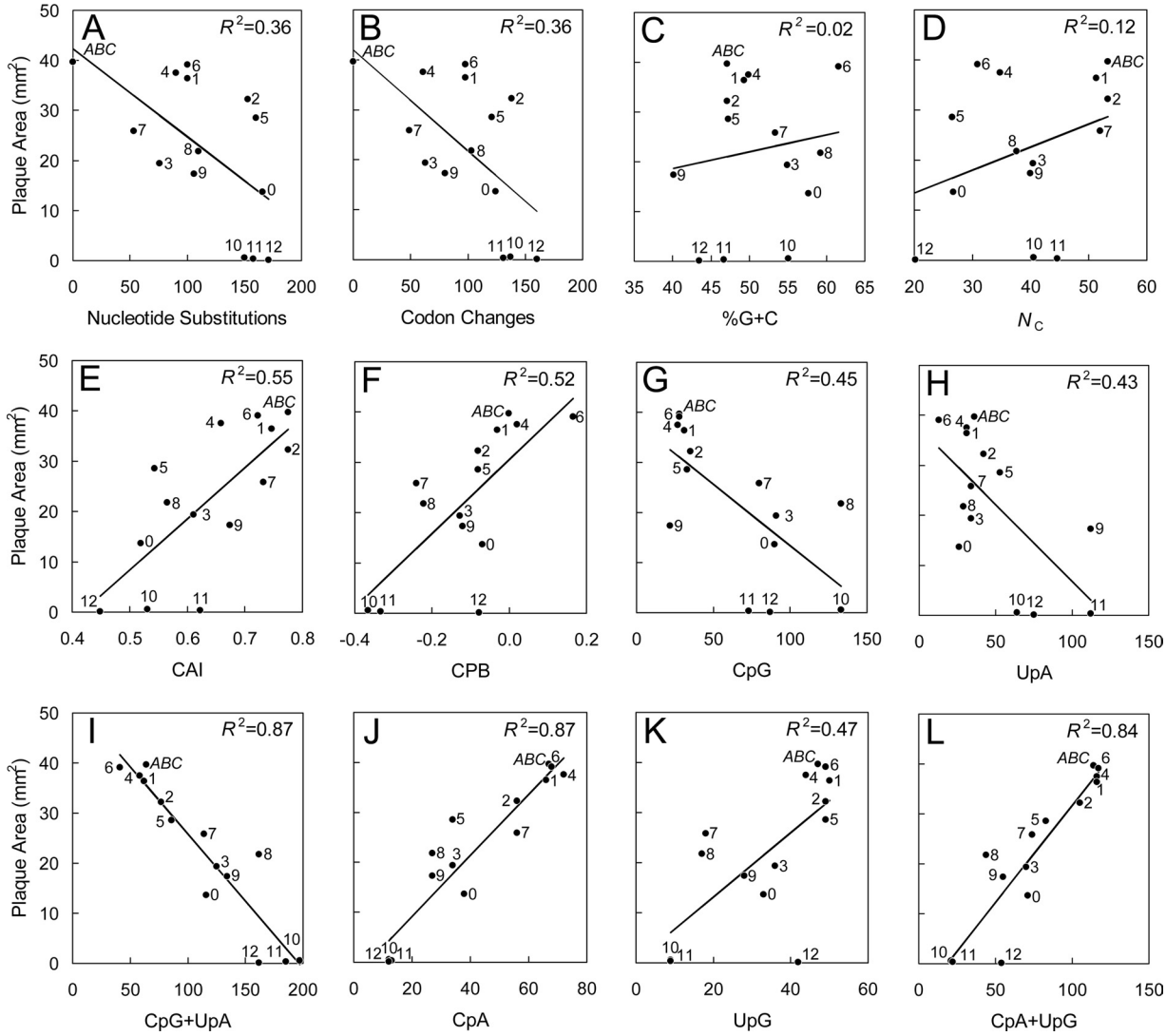

FIG. 4. Mean plaque areas (see Fig. 3A) as a function of different parameters for synonymous codon substitution in cassette *C*, including total nucleotide substitutions (A), total codon changes (B), %G+C (C), effective codon usage (N_C) (D), CAI (E), CPB (F), CpG dinucleotides (G), UpA dinucleotides (H), CpG-plus-UpA dinucleotides (I), CpA dinucleotides (J), UpG dinucleotides (K), and CpA-plus-UpG dinucleotides (L). All virus constructs had unmodified *A* and *B* cassettes. Numbers at data points correspond to cassette *c* subscripts (Table 1).

(data not shown) capsid sequences, gave similar yields of processed virus-specific proteins.

(iv) Temperature sensitivity. Temperature sensitivity is a key phenotypic property of the Sabin OPV strains (33, 36, 41, 59) and other attenuated vaccine strains (3, 45, 56). We measured the temperature sensitivities of virus constructs *ABC*, ABc_0, ABc_{10}, ABc_{11}, ABc_{12}, and abc_0 by determining mean plaque areas (Fig. 8A and B; Table 2) and plaque titers (Fig. 8C; Table 2) on HeLa monolayers incubated at 34.5°C, 37.0°C, and 39.5°C. Mean plaque areas at 65 h of incubation of *ABC*, ABc_0, ABc_{10}, ABc_{11}, and abc_0 were two- to fourfold larger at 37°C than at 34.5°C (Fig. 8A). The exception was ABc_{12}, which had similar plaque areas at both temperatures. However, apart from the unmodified *ABC* virus, which was not temperature sensitive, plaque areas of the codon replacement viruses were three- to eightfold smaller at 39.5°C than at 37°C. The plaque areas shown in Fig. 8B for virus constructs ABc_{10}, ABc_{11}, ABc_{12}, and abc_0 incubated at 39.5°C are likely overestimates, as the monolayers had backgrounds of apparently very minute plaques that were too small and heterogeneous for accurate measurement of their areas (or enumeration). The efficiencies of plating of virus constructs ABc_{10}, ABc_{11}, ABc_{12}, and abc_0 were very low (4 to 7 orders of magnitude lower than those of *ABC* and ABc_0) and decreased by 25-fold (ABc_{11}) to 200-fold (ABc_{12}) from 37°C to 39.5°C (Fig. 8C; Table 2).

(v) Thermostability of virions. The virions of constructs *ABC*, ABc_0, ABc_{10}, ABc_{11}, and abc_0 were found to have retained type- and intratype-specific antigenicities in enzyme-linked immunosorbent assays using highly specific cross-adsorbed antisera (ABc_{12} was also tested, but titers were too low to yield reliable results) (data not shown). To further assess the structural integrities of the assembled virions of the codon replacement constructs, we tested the thermostability of the

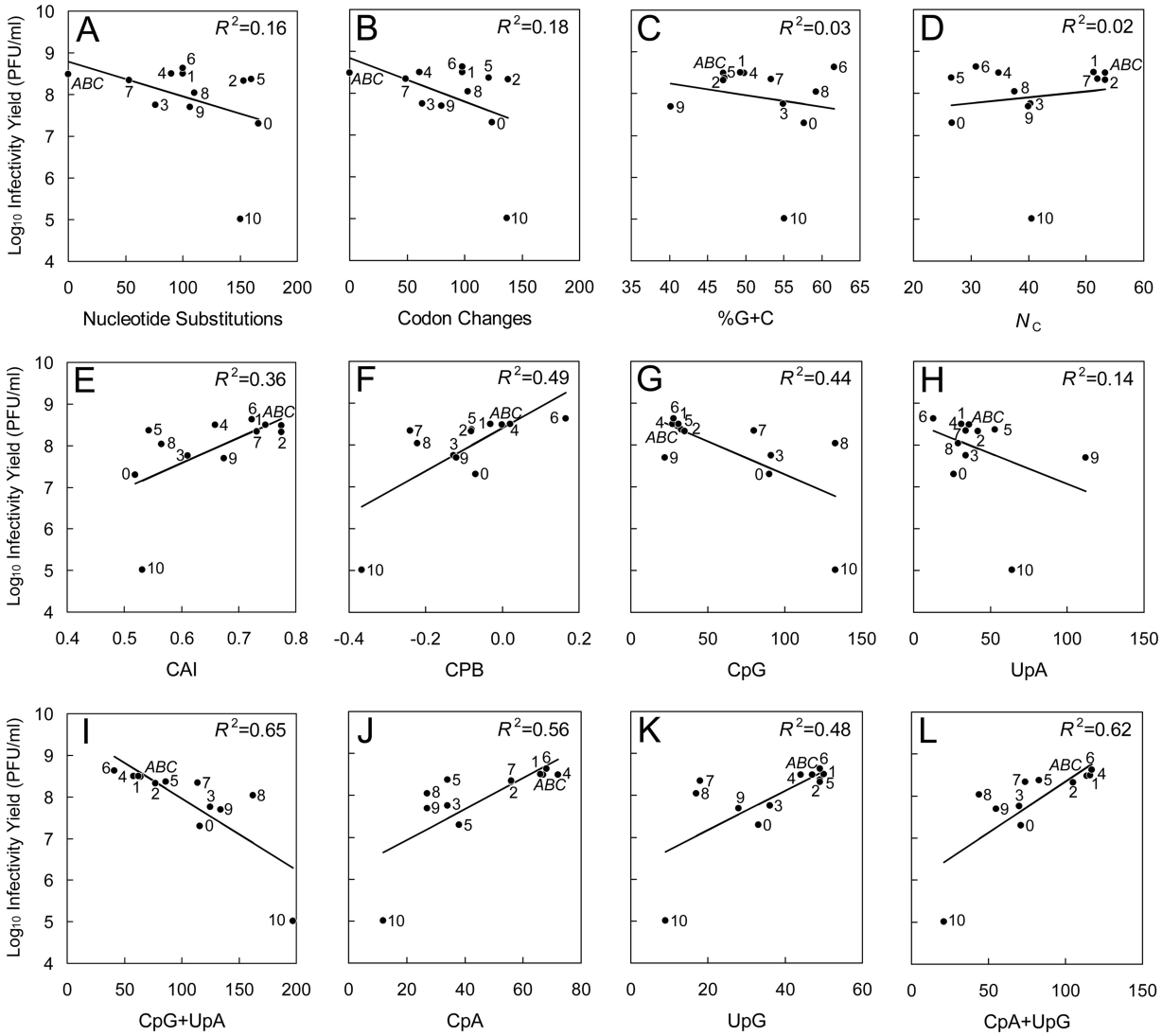

FIG. 5. Virus infectivity yields (averages for 10-h and 12-h time points) in single-step growth experiments (Fig. 3B) as a function of the different parameters for synonymous codon substitution in cassette *C* described in the legend to Fig. 4. Virus constructs ABc_{11} and ABc_{12} were excluded from the single-step growth experiments because their titers were too low for infection at an MOI of 10.

ABC, ABc_0, ABc_{10}, ABc_{11}, ABc_{12}, and abc_0 virions (Fig. 9). Viruses from undiluted clarified infected cell culture lysates were incubated at 46°C, and samples were taken at 0, 5, 10, 20, and 30 min. The kinetics of inactivation of infectivity were similar for *ABC*, ABc_0, ABc_{10}, and ABc_{11}, with an initial rapid 30- to 200-fold decrease in infectivity within the first 5 min followed by slower inactivation kinetics. The observed two-phase thermal inactivation kinetics are typical for poliovirus virions (13, 18) and do not signal any evident virion structural defects. The initial input titer of ABc_{12} was so low that no infectivity was detected after the 0-min time point. Unexpectedly, the inactivation kinetics for abc_0 virions did not show a rapid initial drop, and the overall inactivation rates were similar to those observed at 5 to 30 min for the other constructs (Fig. 9). This effect was reproducible and is under further investigation.

DISCUSSION

The decreased fitness of our codon replacement constructs appears to involve the interaction of several different biological mechanisms. Fitness showed strong inverse correlations with the number and location of CpG and UpA dinucleotides, weaker inverse correlations with the total numbers of nucleotide substitutions and codon changes, and no correlation with N_C. Positive correlations were observed between fitness and the CAI and the CPB score. There appear to be some synergistic effects when high CpG and UpA frequencies are coupled with low N_C and CAI values, as suggested by the very low fitness of construct ABc_{12}, in which CpG and UpA dinucleotides were maximized within cassette *C* codons. Localized increases in %G+C (without increased CpG) to levels well above those found in naturally occurring poliovirus and human enterovirus genomes (43% to 47%) (6) had little effect on

TABLE 2. Phenotypic properties of codon replacement virus constructs

Virus construct[a]	Relative plaque area (A/A_{ABC})[b]	Relative plaque yield (at 37°C)[c]	Specific infectivity (particles/PFU)[d,e]	Plaque area at 39.5°C/ plaque area at 37°C[f]	Plaque yield at 39.5°C/ plaque yield at 37°C[e,f]
ABC	1.000	1.00	148	0.75	0.821
ABc_0	0.344	0.07	371	0.22	0.897
ABc_1	0.918	0.19	ND	ND	ND
ABc_2	0.813	1.02	ND	ND	ND
ABc_3	0.488	0.76	ND	ND	ND
ABc_4	0.945	1.03	ND	ND	ND
ABc_5	0.719	0.69	ND	ND	ND
ABc_6	0.985	1.39	ND	ND	ND
ABc_7	0.651	0.72	ND	ND	ND
ABc_8	0.549	0.36	ND	ND	ND
ABc_9	0.436	0.16	ND	ND	ND
ABc_{10}	0.015	<0.01	1,040	0.18	0.039
ABc_{11}	0.008	ND[g]	6,250	0.13	0.040
ABc_{12}	0.002	ND[g]	62,000	0.34	0.005
abc_0	0.013	<0.01	16,700	0.17	0.026

[a] Construct properties are summarized in Table 1; construct abc_0 is also described in Fig. 1.

[b] A_{ABC}, mean area of *ABC* plaque (40 mm^2). Plaque areas were measured on HeLa monolayers after incubation at 37°C for 65 h.

[c] Plaque yields (averages for 10-h and 12-h time points) were determined in the single-step growth experiments shown in Fig. 3.

[d] Specific infectivities were determined with virions purified from infected RD cells.

[e] ND, not determined.

[f] Temperature sensitivity was measured by incubation of virus stocks and determination of ratios of plaque yields on HeLa cells at 39.5°C and 37.0°C.

[g] Not determined because original infectivity yields of ABc_{11} and ABc_{12} were too low for use as input virus at an MOI of 10 in single-step growth experiments.

fitness. Replacement in cassette *C* of MEF-1 capsid codons with Lansing codons or our randomization of the natural MEF-1 synonymous codons (both replacements incorporated only small changes in CpG and UpA frequencies) also had minimal biological effects.

Decreased translational efficiency does not appear to be the main physiological defect in our codon replacement constructs, despite the large-scale use of unpreferred codons. In our previous (8) and current experiments, virus constructs with widely varying infectivities produced similar levels of virus-specific proteins in infected cells. Although it could be argued that translation is so tightly coupled to critical steps in the poliovirus replication cycle that small deficits in translation could cause disproportionately large decreases in virus infectivities, other observations counter this view. For example, an approximately four- to eightfold decrease in translational efficiency in type 1 poliovirus was associated with only a proportionate reduction in plaque yields (21).

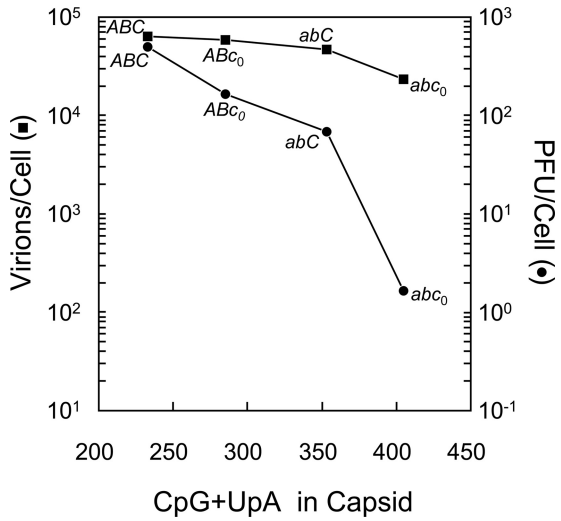

FIG. 6. Virus particle yields (solid squares) and infectivity yields (PFU/cell; solid circles) of virus constructs *ABC*, ABc_0, *abC*, and abc_0 in RD cells as a function of the total number of CpG-plus-UpA dinucleotides in the capsid region.

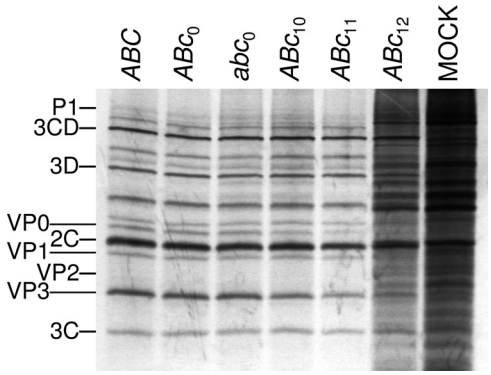

FIG. 7. SDS-PAGE analysis of poliovirus-specific proteins produced by *ABC*, ABc_0, abc_0, ABc_{10}, ABc_{11}, and ABc_{12} viruses in vivo. Lysates were obtained from HeLa cells infected with purified virus (MOI = 25 PFU/cell) labeled with [^{35}S]methionine at 4 to 7 h postinfection. Noncapsid proteins were identified by their electrophoretic mobilities and band intensities; capsid proteins were identified by their comigration with proteins from purified virions.

Suppression of CpG is strong in vertebrates (4, 37) and their single-stranded RNA viruses (19, 28, 49), including poliovirus (47, 50), and suppression of UpA is virtually universal (4, 37). The initial evidence pointing to the negative effects of increased CpG and UpA on poliovirus fitness was the observation that revertants selected during serial passage of codon-deoptimized constructs of Sabin 2 (8) and MEF-1 (R. Campagnoli, unpublished results) had high frequencies of mutations that eliminated CpG and UpA. Many of these reversions involved fixation of amino acid replacements in normally conserved capsid sites (8, 25). The properties of the MEF-1 constructs described here provide direct confirmation of fitness reductions associated with increased frequencies of CpG and UpA dinucleotides.

The importance of CpG and UpA frequencies to poliovirus fitness is reinforced by the recent report of Coleman et al. (13), who replaced the natural capsid region codon pairs of poliovirus type 1 (Mahoney strain) with synonymous codon pairs rarely found in the open reading frames of human genes. The biochemical properties of their constructs, especially the low specific infectivities, were similar to those described here for MEF-1 and previously for Sabin 2 (8) and strain Mahoney (38). Their constructs were attenuated for Tg21 transgenic mice expressing the CD155 PVR and could induce protective immunity against subsequent challenge with neurovirulent wild-type Mahoney virus. A prominent feature of the most disfavored codon pairs is the presence of CpG or UpA across

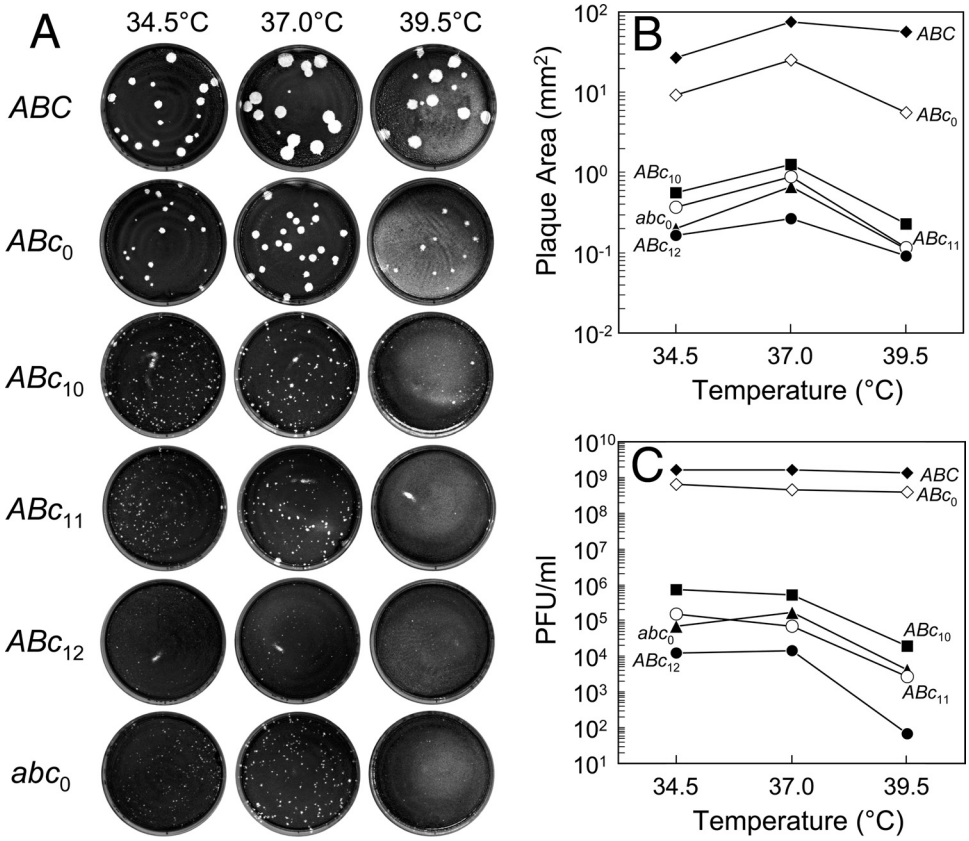

FIG. 8. Temperature sensitivities of codon replacement virus constructs. Plaque morphologies (A), mean plaque areas (B), and plaque titers (C) are shown for constructs *ABC*, ABc_0, ABc_{10}, ABc_{11}, ABc_{12}, and abc_0 incubated on HeLa cell monolayers at 34.5°C, 37.0°C, and 39.5°C. Relative amounts of infected cell culture lysates yielding the plaques shown in each dish at 34.5°C, 37.0°C, and 39.5°C, respectively, were as follows: *ABC*, 1, 1, 1; ABc_0, 10, 10, 10; ABc_{10}, 10^4, 10^4, 10^6; ABc_{11}, 10^5, 10^5, 10^6; ABc_{12}, 10^6, 10^6, 10^8; and abc_0, 10^4, 10^4, 10^6.

codons (13). Thus, the observed CPB in poliovirus and in humans and higher eukaryotes may be driven primarily by CpG and UpA dinucleotide suppression (4, 37). In this context, it is notable that in cassette *C* of the construct with the lowest fitness, ABc_{12}, within-codon CpG and UpA frequencies were maximized but the CPB score was similar to those of higher-fitness constructs, including *ABC*.

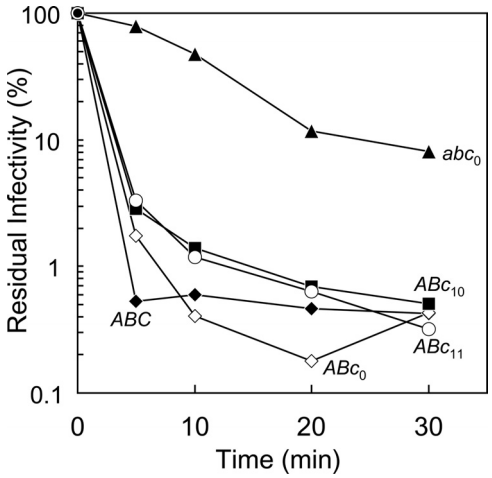

FIG. 9. Thermal inactivation kinetics of *ABC*, ABc_0, abc_0, ABc_{10}, ABc_{11}, and ABc_{12} virus constructs at 46°C. Input titers (PFU/ml) were 4.0×10^9 (*ABC*), 6.4×10^8 (ABc_0), 2.6×10^7 (abc_0), 6.9×10^6 (ABc_{10}), 7.1×10^5 (ABc_{11}), and 1.5×10^4 (ABc_{12}). The infectivity of ABc_{12} was below detectable levels at 5 min of incubation at 46°C.

The underlying drivers of suppression appear to differ between CpG and UpA, although in both instances selection appears to act primarily through genome-wide mutational processes, and only secondarily on translated sequences (4, 11). In vertebrate genomes, most CpG dinucleotides are methylated at position 5 of cytosine, and spontaneous deamination of 5-methylcytosine results in a TpG mutation (and a CpA mutation on the complementary strand). Suppression of CpG in vertebrate DNA has been attributed to selection against potential mutational hot spots (4), but this explanation does not account for suppression of CpG in the genomes of single-stranded RNA viruses where cytosine is not 5-methylated (28, 49). Another possible mechanism for CpG suppression is that unmethylated CpG in DNA stimulates the innate immune system via the Toll-like receptor TLR9 (62), and RNA viruses may have evolved to evade the innate immune system by mimicking the dinucleotide patterns of host cell genes and mRNAs (19). In addition, some RNA oligonucleotide motifs containing unmethylated CpGs are directly immunostimulatory via pathways distinct from TLR9 (58) and therefore may be subject to negative selection.

UpA dinucleotides, in contrast, are direct substrates for cleavage of single-stranded RNA by endoribonucleases (4, 17,

46), including the antiviral RNase L (22, 66). Rates of RNA degradation may increase in templates rich in UpA and decrease in homologous templates rich in CpG (17). The differing biochemical mechanisms underlying CpG and UpA suppression may shape the strategy for optimal design of codon-deoptimized virus constructs.

As previously suggested (8, 13, 38), codon deoptimization may offer a systematic general approach to the development of RNA virus vaccines with very high genetic stabilities. Moreover, because all substitutions are synonymous, surface antigens remain unaltered. The basic strategy is to modulate fitness along a shallow fitness gradient, thereby maximizing the number of substitutions contributing to the desired phenotypes. If selection coefficients at individual sites are low, full phenotypic reversion would require many incremental steps occurring over many rounds of replication. The distribution of attenuating substitutions over numerous sites contrasts with the properties of the Sabin OPV strains, where the key attenuating substitutions are localized to two to six sites (5, 29, 34, 48, 63, 67). For poliovirus, the most immediate need is for safer IPV seed strains suitable for posteradication vaccine production in developing countries (12, 15). Genetic inactivation of infectivity by incorporation of CpG and UpA dinucleotides into synonymous capsid region codons may lead to improved poliovirus vaccine strains having antigenic properties identical to those of the current vaccine strains.

ACKNOWLEDGMENTS

We thank Deborah Moore, A. J. Williams, and Naomi Dybdahl-Sissoko for characterizing the antigenic properties of virus constructs, Harrie van der Avoort for providing us with the specific cross-adsorbed antisera, and Brian Holloway and Melissa Olsen-Rasmussen for preparing the synthetic deoxyoligonucleotides used in this study.

The findings and conclusions in this report are those of the authors and do not necessarily represent the views of the funding agency.

REFERENCES

1. **André, S., B. Seed, J. Eberle, W. Schraut, A. Bültmann, and J. Haas.** 1998. Increased immune response elicited by DNA vaccination with a synthetic gp120 sequence with optimized codon usage. J. Virol. **72:**1497–1503.
2. **Arnold, J. J., and C. E. Cameron.** 2004. Poliovirus RNA-dependent RNA polymerase ($3D^{pol}$): pre-steady-state kinetic analysis of ribonucleotide incorporation in the presence of Mg^{2+}. Biochemistry **43:**5126–5137.
3. **Belshe, R. B., R. Walker, J. J. Stoddard, G. Kemble, H. F. Maassab, and P. M. Mendelman.** 2008. Influenza vaccine—live, p. 291–309. *In* S. A. Plotkin, W. A. Orenstein, and P. A. Offit (ed.), Vaccines, 5th ed. W. B. Saunders Company, Philadelphia, PA.
4. **Beutler, E., T. Gelbart, J. H. Han, J. A. Koziol, and B. Beutler.** 1989. Evolution of the genome and the genetic code: selection at the dinucleotide level by methylation and polyribonucleotide cleavage. Proc. Natl. Acad. Sci. USA **86:**192–196.
5. **Bouchard, M. J., D. H. Lam, and V. R. Racaniello.** 1995. Determinants of attenuation and temperature sensitivity in the type 1 poliovirus Sabin strain. J. Virol. **69:**4972–4978.
6. **Brown, B. A., M. S. Oberste, K. Maher, and M. Pallansch.** 2003. Complete genomic sequencing shows that polioviruses and members of human enterovirus species C are closely related in the non-capsid coding region. J. Virol. **77:**8973–8984.
7. **Burge, C., A. M. Campbell, and S. Karlin.** 1992. Over- and under-representation of short oligonucleotides in DNA sequences. Proc. Natl. Acad. Sci. USA **89:**1358–1362.
8. **Burns, C. C., J. Shaw, R. Campagnoli, J. Jorba, A. Vincent, J. Quay, and O. M. Kew.** 2006. Modulation of poliovirus replicative fitness in HeLa cells by deoptimization of synonymous codon usage in the capsid region. J. Virol. **80:**3259–3272.
9. **Cello, J., A. V. Paul, and E. Wimmer.** 2002. Chemical synthesis of poliovirus cDNA: generation of infectious virus in the absence of natural template. Science **297:**1016–1018.
10. **Centers for Disease Control and Prevention.** 2007. Update on vaccine-derived polioviruses—worldwide, January 2006–August 2007. MMWR Morb. Mortal. Wkly. Rep. **56:**996–1001.
11. **Chen, S. L., W. Lee, A. K. Hottes, L. Shapiro, and H. H. McAdams.** 2004. Codon usage between genomes is constrained by genome-wide mutational processes. Proc. Natl. Acad. Sci. USA **101:**3480–3485.
12. **Chumakov, K., and E. Ehrenfeld.** 2008. New generation of inactivated poliovirus vaccines for universal immunization after eradication of poliomyelitis. Clin. Infect. Dis. **47:**1587–1592.
13. **Coleman, J. R., D. Papamichail, S. Skiena, B. Futcher, E. Wimmer, and S. Mueller.** 2008. Virus attenuation by genome-scale changes in codon pair bias. Science **320:**1784–1787.
14. **de la Torre, J. C., C. Giachetti, B. L. Semler, and J. J. Holland.** 1992. High frequency of single-base transitions and extreme frequency of precise multiple-base reversion mutations in poliovirus. Proc. Natl. Acad. Sci. USA **89:**2531–2535.
15. **Deshpande, J. M., S. S. Nadkarni, and Z. A. Siddiqui.** 2003. Detection of MEF-1 laboratory reference strain of poliovirus type 2 in children with poliomyelitis in India in 2002 and 2003. Indian J. Med. Res. **118:**217–223.
16. **Domingo, E., E. Baranowski, C. Escarmís, F. Sobrino, and J. J. Holland.** 2002. Error frequencies of picornavirus RNA polymerases: evolutionary implications for virus populations, p. 285–298. *In* B. L. Semler and E. Wimmer (ed.), Molecular biology of picornaviruses. ASM Press, Washington, DC.
17. **Duan, J., and M. A. Antezana.** 2003. Mammalian mutation pressure, synonymous codon choice, and mRNA degradation. J. Mol. Evol. **57:**694–701.
18. **French, R. C., and R. E. Armstrong.** 1960. Thermal inactivation of MEF1 poliovirus. Can. J. Microbiol. **6:**175–181.
19. **Greenbaum, B. D., A. J. Levine, G. Bhanot, and R. Rabadan.** 2008. Patterns of evolution and host gene mimicry in influenza and other RNA viruses. PLoS Pathog. **4:**e1000079.
20. **Guillot, S., V. Caro, N. Cuervo, E. Korotkova, M. Combiescu, A. Persu, A. Aubert-Combiescu, F. Delpeyroux, and R. Crainic.** 2000. Natural genetic exchanges between vaccine and wild poliovirus strains in humans. J. Virol. **74:**8434–8443.
21. **Haller, A. A., S. R. Stewart, and B. L. Semler.** 1996. Attenuation stem-loop lesions in the 5′ noncoding region of poliovirus RNA: neuronal cell-specific translation defects. J. Virol. **70:**1467–1474.
22. **Han, J.-Q., H. L. Townsend, B. K. Jha, J. M. Paranjape, R. H. Silverman, and D. J. Barton.** 2007. A phylogenetically conserved RNA structure in the poliovirus open reading frame inhibits the antiviral endoribonuclease RNase L. J. Virol. **81:**5561–5572.
23. **He, Y.-N., V. D. Bowman, S. Mueller, C. M. Bator, J. Bella, X.-H. Peng, T. S. Baker, E. Wimmer, R. J. Kuhn, and M. G. Rossmann.** 2000. Interaction of the poliovirus receptor with poliovirus. Proc. Natl. Acad. Sci. USA **97:**79–84.
24. **Jenkins, G. M., and E. C. Holmes.** 2003. The extent of codon usage bias in human RNA viruses and its evolutionary origin. Virus Res. **92:**1–7.
25. **Jorba, J., R. Campagnoli, L. De, and O. Kew.** 2008. Calibration of multiple poliovirus molecular clocks covering an extended evolutionary range. J. Virol. **82:**4429–4440.
26. **Josse, J., A. D. Kaiser, and A. Kornberg.** 1961. Enzymatic synthesis of deoxyribonucleic acid. VIII. Frequencies of nearest neighbor base sequences in deoxyribonucleic acid. J. Biol. Chem. **236:**864–875.
27. **Kane, J. F.** 1995. Effects of rare codon clusters on high-level expression of heterologous proteins in Escherichia coli. Curr. Opin. Biotechnol. **6:**494–500.
28. **Karlin, S., W. Doerfler, and L. R. Cardon.** 1994. Why is CpG suppressed in the genomes of virtually all small eukaryotic viruses but not in those of large eukaryotic viruses? J. Virol. **68:**2889–2897.
29. **Kawamura, N., M. Kohara, S. Abe, T. Komatsu, K. Tago, M. Arita, and A. Nomoto.** 1989. Determinants in the 5′ noncoding region of poliovirus Sabin 1 RNA that influence the attenuation phenotype. J. Virol. **63:**1302–1309.
30. **Kew, O. M., V. Morris-Glasgow, M. Landaverde, C. Burns, J. Shaw, Z. Garib, J. André, E. Blackman, C. J. Freeman, J. Jorba, R. Sutter, G. Tambini, L. Venczel, C. Pedreira, F. Laender, H. Shimizu, T. Yoneyama, T. Miyamura, H. van der Avoort, M. S. Oberste, D. Kilpatrick, S. Cochi, M. Pallansch, and C. de Quadros.** 2002. Outbreak of poliomyelitis in Hispaniola associated with circulating type 1 vaccine-derived poliovirus. Science **296:**356–359.
31. **Kew, O. M., R. W. Sutter, E. M. de Gourville, W. R. Dowdle, and M. A. Pallansch.** 2005. Vaccine-derived polioviruses and the endgame strategy for global polio eradication. Annu. Rev. Microbiol. **59:**587–635.
32. **Liu, H.-M., D.-P. Zheng, L.-B. Zhang, M. S. Oberste, O. M. Kew, and M. A. Pallansch.** 2003. Serial recombination during circulation of type 1 wild-vaccine recombinant polioviruses in China. J. Virol. **77:**10994–11005.
33. **Macadam, A. J., G. Ferguson, D. M. Stone, J. Meredith, S. Knowlson, G. Auda, J. W. Almond, and P. D. Minor.** 2006. Rational design of genetically stable, live-attenuated poliovirus vaccines of all three serotypes: relevance to poliomyelitis eradication. J. Virol. **80:**8653–8663.
34. **Macadam, A. J., S. R. Pollard, G. Ferguson, R. Skuce, D. Wood, J. W. Almond, and P. D. Minor.** 1993. Genetic basis of attenuation of the Sabin type 2 vaccine strain of poliovirus in primates. Virology **192:**18–26.
35. **Minor, P. D.** 1990. Antigenic structure of picornaviruses. Curr. Top. Microbiol. Immunol. **161:**121–154.
36. **Minor, P. D., G. Dunn, D. M. A. Evans, D. I. Magrath, A. John, J. Howlett, A. Phillips, G. Westrop, K. Wareham, J. W. Almond, and J. M. Hogle.** 1989.

The temperature sensitivity of the Sabin type 3 vaccine strain of poliovirus: molecular and structural effects of a mutation in the capsid protein VP3. J. Gen. Virol. **70:**1117–1123.
37. **Moura, G., M. Pinheiro, J. Arrais, A. C. Gomes, L. Carreto, A. Freitas, J. L. Oliveira, and M. A. S. Santos.** 2007. Large scale comparative codon-pair context analysis unveils general rules that fine-tune evolution of mRNA primary structure. PLoS One **2:**e847.
38. **Mueller, S., D. Papamichail, J. R. Coleman, S. Skiena, and E. Wimmer.** 2006. Reduction of the rate of poliovirus protein synthesis through large-scale codon deoptimization causes attenuation of viral virulence by lowering specific infectivity. J. Virol. **80:**9687–9696.
39. **Nakamura, Y., T. Gojobori, and T. Ikemura.** 2000. Codon usage tabulated from international DNA sequence databases: status for the year 2000. Nucleic Acids Res. **28:**292.
40. **Nottay, B. K., O. M. Kew, M. H. Hatch, J. T. Heyward, and J. F. Obijeski.** 1981. Molecular variation of type 1 vaccine-related and wild polioviruses during replication in humans. Virology **108:**405–423.
41. **Omata, T., M. Kohara, S. Kuge, T. Komatsu, S. Abe, B. L. Semler, A. Kameda, H. Itoh, M. Arita, E. Wimmer, and A. Nomoto.** 1986. Genetic analysis of the attenuation phenotype of poliovirus type 1. J. Virol. **58:**348–358.
42. **Palmenberg, A. C., and J.-Y. Sgro.** 1997. Topological organization of picornaviral genomes: statistical prediction of RNA structural signals. Semin. Virol. **8:**231–241.
43. **Pinheiro, M., V. Afreixo, G. Moura, A. Freitas, M. A. Santos, J. L. Oliveira, and M. A. S. Santos.** 2006. Statistical, computational and visualization methodologies to unveil gene primary structure features. Methods Inf. Med. **45:**163–168.
44. **Pipkin, P. A., D. J. Wood, V. R. Racaniello, and P. D. Minor.** 1993. Characterisation of L cells expressing the human poliovirus receptor for the specific detection of polioviruses in vitro. J. Virol. Methods **41:**333–340.
45. **Plotkin, S. A., and S. E. Reef.** 2008. Rubella vaccine, p. 735–771. *In* S. A. Plotkin, W. A. Orenstein, and P. A. Offit (ed.), Vaccines, 5th ed. W. B. Saunders Company, Philadelphia, PA.
46. **Qiu, L., A. Moreira, G. Kaplan, R. Levitz, J. Y. Wang, C. Xu, and K. Drlica.** 1998. Degradation of hammerhead ribozymes by human ribonucleases. Mol. Gen. Genet. **258:**352–362.
47. **Racaniello, V. R., and D. Baltimore.** 1981. Molecular cloning of poliovirus cDNA and determination of the complete nucleotide sequence of the viral genome. Proc. Natl. Acad. Sci. USA **78:**4887–4891.
48. **Ren, R., E. G. Moss, and V. R. Racaniello.** 1991. Identification of two determinants that attenuate vaccine-related type 2 poliovirus. J. Virol. **65:** 1377–1382.
49. **Rima, B. K., and N. V. McFerran.** 1997. Dinucleotide and stop codon frequencies in single-stranded RNA viruses. J. Gen. Virol. **78:**2859–2870.
50. **Rothberg, P. G., and E. Wimmer.** 1981. Mononucleotide and dinucleotide frequencies, and codon usage in poliovirion RNA. Nucleic Acids Res. **9:**6221–6229.
51. **Rueckert, R. R.** 1976. On the structure and morphogenesis of picornaviruses, p. 131–213. *In* H. Fraenkel-Conrat and R. R. Wagner (ed.), Comprehensive virology, vol. 6. Plenum Press, New York, NY.
52. **Schlesinger, R. W., I. M. Morgan, and P. K. Olitsky.** 1943. Transmission to rodents of Lansing type poliomyelitis virus originating from the Middle East. Science **98:**452–454.
53. **Sharp, P. M., and W. H. Li.** 1987. The codon adaptation index—a measure of directional synonymous codon usage bias, and its potential applications. Nucleic Acids Res. **15:**1281–1295.
54. **Simmonds, P., A. Tuplin, and D. J. Evans.** 2004. Detection of genome-scale ordered RNA structure (GORS) in genomes of positive-stranded RNA viruses: implications for virus evolution and host persistence. RNA **10:**1337–1351.
55. **Stemmer, W. P. C., A. Crameri, K. D. Ha, T. M. Brennan, and H. L. Heyneker.** 1995. Single-step assembly of a gene and entire plasmid from large numbers of oligodeoxyribonucleotides. Gene **164:**49–53.
56. **Strebel, P. M., M. J. Papania, G. H. Dayan, and N. A. Halsey.** 2008. Measles vaccine, p. 353–398. *In* S. A. Plotkin, W. A. Orenstein, and P. A. Offit (ed.), Vaccines, 5th ed. W. B. Saunders Company, Philadelphia, PA.
57. **Strebel, P. M., R. W. Sutter, S. L. Cochi, R. J. Biellik, E. W. Brink, O. M. Kew, M. A. Pallansch, W. A. Orenstein, and A. R. Hinman.** 1992. Epidemiology of poliomyelitis in the United States one decade after the last reported case of indigenous wild virus-associated disease. Clin. Infect. Dis. **14:**568–579.
58. **Sugiyama, T., M. Gursel, F. Takeshita, C. Coban, J. Conover, T. Kaisho, S. Akira, D. M. Klinman, and K. J. Ishii.** 2005. CpG RNA: identification of novel single-stranded RNA that stimulates human CD14+CD11c+ monocytes. J. Immunol. **174:**2273–2279.
59. **Sutter, R. W., O. M. Kew, and S. L. Cochi.** 2008. Poliovirus vaccine—live, p. 631–685. *In* S. A. Plotkin, W. A. Orenstein, and P. A. Offit (ed.), Vaccines, 5th ed. W. B. Saunders Company, Philadelphia, PA.
60. **Sutter, R. W., and R. Prevots.** 1994. Vaccine-associated paralytic poliomyelitis among immunodeficient persons. Infect. Med. **11:**426–438.
61. **Swartz, M. N., T. A. Trautner, and A. Kornberg.** 1962. Enzymatic synthesis of deoxyribonucleic acid. XI. Further studies on nearest neighbor base sequences in deoxyribonucleic acids. J. Biol. Chem. **237:**1961–1967.
62. **Takeshita, F., I. Gursel, K. J. Ishii, K. Suzuki, M. Gursel, and D. M. Klinman.** 2004. Signal transduction pathways mediated by the interaction of CpG DNA with Toll-like receptor 9. Semin. Immunol. **16:**17–22.
63. **Tardy-Panit, M., B. Blondel, A. Martin, F. Tekaia, F. Horaud, and F. Delpeyroux.** 1993. A mutation in the RNA polymerase of poliovirus type 1 contributes to attenuation in mice. J. Virol. **67:**4630–4638.
64. **van der Avoort, H. G. A. M., B. P. Hull, T. Hovi, M. A. Pallansch, O. M. Kew, R. Crainic, D. J. Wood, M. N. Mulders, and A. M. van Loon.** 1995. A comparative study of five methods of intratypic differentiation of polioviruses. J. Clin. Microbiol. **33:**2562–2566.
65. **Ward, C. D., and J. B. Flanegan.** 1992. Determination of the poliovirus RNA polymerase error frequency at eight sites in the viral genome. J. Virol. **66:**3784–3793.
66. **Washenberger, C. L., J.-Q. Han, K. J. Kechris, B. K. Jha, R. H. Silverman, and D. J. Barton.** 2007. Hepatitis C virus RNA: dinucleotide frequencies and cleavage by RNase L. Virus Res. **130:**85–95.
67. **Westrop, G. D., K. A. Wareham, D. M. Evans, G. Dunn, P. D. Minor, D. I. Magrath, F. Taffs, S. Marsden, M. A. Skinner, G. C. Schild, and J. W. Almond.** 1989. Genetic basis of attenuation of the Sabin type 3 oral poliovirus vaccine. J. Virol. **63:**1338–1344.
68. **Witwer, C., S. Rauscher, I. L. Hofacker, and P. F. Stadler.** 2001. Conserved RNA secondary structures in *Picornaviridae* genomes. Nucleic Acids Res. **29:**5079–5089.
69. **Wright, F.** 1990. The effective number of codons used in a gene. Gene **87:**23–29.
70. **Yadava, A., and C. F. Ockenhouse.** 2003. Effect of codon optimization on expression levels of a functionally folded malaria vaccine candidate in prokaryotic and eukaryotic expression systems. Infect. Immun. **71:**4961–4969.
71. **Yang, C.-F., T. Naguib, S.-J. Yang, E. Nasr, J. Jorba, N. Ahmed, R. Campagnoli, H. van der Avoort, H. Shimizu, T. Yoneyama, T. Miyamura, M. A. Pallansch, and O. Kew.** 2003. Circulation of endemic type 2 vaccine-derived poliovirus in Egypt, 1983 to 1993. J. Virol. **77:**8366–8377.